

Cold equation of state from Thomas-Fermi-Dirac-Weizsacker theory

Andrew M. Abrahams and Stuart L. Shapiro*

Center for Radiophysics and Space Research, Cornell University, Ithaca, New York 14853

(Received 5 February 1990; revised manuscript received 4 May 1990)

The Thomas-Fermi-Dirac (TFD) electronic structure model with the Weizsacker gradient corrections (TFD- λ W) is employed to calculate the cold equation of state in the Wigner-Seitz spherical-cell approximation. We demonstrate how inclusion of the Weizsacker term removes many of the unphysical features of the TFD lattice model. Results are summarized for seven elements: $^{12}_6\text{C}$, $^{24}_{12}\text{Mg}$, $^{56}_{26}\text{Fe}$, $^{108}_{47}\text{Ag}$, $^{197}_{79}\text{Au}$, $^{207}_{82}\text{Pb}$, and $^{236}_{92}\text{U}$. Our equation of state (computed using several values of the Weizsacker coupling coefficient) is compared with previous computations and with experimental data. The Weizsacker correction substantially improves the theoretical TFD equation of state at low densities. We also calculate low-mass, equilibrium stellar models constructed from the TFD- λ W equation of state for carbon. We find that for $\lambda = \frac{1}{9}$ the maximum radius of a carbon white dwarf star is $R/R_\odot = 3.9 \times 10^{-2}$ at a mass $M/M_\odot = 2.3 \times 10^{-3}$.

I. INTRODUCTION

Thomas-Fermi (TF) and Thomas-Fermi-Dirac (TFD) models have been essential tools in the study of many electron systems such as atoms, molecules, and solids since their conception in the 1920s and 1930s. Recently, density-functional theory has provided a rigorous mathematical basis for these approximations¹ and it has been shown² that TF is identical to the exact quantum theory, based on the Schrödinger equation, in the limit of large nuclear charge ($Z \rightarrow \infty$). In the TF theory, electronic wave functions are assumed to be locally planar. This provides a density-functional kinetic energy which, along with the classical potential energy of electron-electron and electron-nucleus Coulomb interactions, forms the TF energy functional. In TFD theory an additional term is added, also based on the plane-wave approximation that represents the exchange part of the potential energy.³

There are several well-known physical defects with the atomic models found using TF and TFD theory. In these models the electron density blows up to infinity as $r \rightarrow 0$, i.e., at the nucleus, where it should be finite. In addition, the electron density has a power-law tail rather than the required exponential falloff as $r \rightarrow \infty$. A further unphysical feature of TFD model atoms is that they must be truncated at finite radii.⁴ Another very serious problem is the *no-binding theorem*, by which molecules are impossible. Originally proposed by Teller, this theorem was rigorously proven by Balazs⁵ in the special case of a diatomic molecule and more generally by Lieb and Simon.⁶

Weizsacker⁴ sought to remedy some of these defects by allowing the electron wavefunctions to be modified plane waves. In the resulting TFD- λ W theory a gradient term is introduced into the kinetic energy functional with coefficient λ (Weizsacker derived the term originally with coupling coefficient $\lambda=1$). In TFD- λ W theory atoms have electronic structures in reasonable qualitative agreement with quantum mechanical predictions.² The electron density approaches a finite density at the nucleus

and falls off exponentially far from the nucleus. Most significantly, binding of atoms can occur so that molecules are possible.

The Weizsacker correction has been formally justified by a number of authors on the basis of gradient expansions (see discussion and references in Parr and Yang¹ and Lieb²). This technique truncated at second order leads to a value of $\lambda = \frac{1}{9}$ for the Weizsacker coupling coefficient. Yang⁸ confirms this result with a path integral derivation of the first-order density matrix. There are other frequently cited values of λ arising both from semiempirical and theoretical considerations. Yonei and Tomishima quote a value of $\lambda \approx \frac{1}{5}$, first based on numerical solutions of atomic models without electron-electron repulsion⁹ and then based on solutions of the full TFD- λ W equation compared with Hartree-Fock calculations of the total energy for neutral, closed-shell atoms.¹⁰ Lieb² does a large- Z analysis of the TFD- λ W theory for atoms and arrives at $\lambda \approx 0.186$ However, there is no theoretical justification for using this particular value for calculations of atoms under pressure.

Jones and Young¹¹ use the linear response function for a uniform electron gas to argue that the Weizsacker coefficient should be $\frac{1}{9}$ for long-wavelength perturbations (high electron density) and 1 in the short-wavelength limit (low electron density). An explicit form for λ as a function of density was found by Kahn and Ying¹² by fitting to induced dipole moment data. Another choice of λ is discussed by Brack¹³ who attempts to incorporate higher-order effects (from the gradient expansion) and discusses $\lambda \approx 1.4/9 - 1.5/9$. Other numerical solutions to the full TFD- λ W equation have been found by Stich *et al.*,¹⁴ for neutral atoms and positive ions. Yang⁸ solves the equation for rare-gas atoms for a variety of values of λ . Engel and Dreizler¹⁵ derive a relativistic version of the TFD- λ W equation with $\lambda = \frac{1}{9}$ and solve it for neutral atoms and positive ions. This analysis is extended¹⁶ to include external, time-independent electric and magnetic fields. There also exist approximate solutions for diatomic molecules.¹⁷

The crucial ingredient for building models of planets, brown dwarfs, and cold white dwarfs is the equation of state for cold, degenerate matter.¹⁸ Feynman, Metropolis, and Teller¹⁹ (hereafter FMT) used both the TF and TFD models to construct equations of state at high pressure. They adopted the familiar Wigner-Seitz approximation to calculate the electronic structure. In this approximation the actual lattice cell is replaced by a neutral sphere consisting of a cloud of Z electrons surrounding a point ion of charge Z at the center. Adjacent cells do not interact with each other. FMT implement this spherical cell model by replacing the zero pressure condition used to establish the surface of the free TFD atom with the condition that the gradient of the total electrical potential (i.e., the electric field) be zero at the cell boundaries. To generate an equation of state, the matter density is varied by changing the cell size, and the resulting pressure is obtained from the value of the potential at the cell surface (see Sec. II). They performed this calculation for several values of Z , supplementing the work of Slater and Krutter and of Jensen.²⁰ A similar computation for ^{56}Fe is given by Harrison *et al.*,²¹ who use the equation of state to construct zero-temperature white-dwarf models.

A refinement of the pioneering FMT calculation was performed by Salpeter and Zapolsky.²² They attempt to correct the considerable errors in the TFD pressure-density relation for heavy elements at low pressures by adding a correlation energy correction. Using the results of field-theoretical calculations of Gell-Mann and Brueckner²³ for the correlation energy of a high-density, homogeneous electron gas, Salpeter and Zapolsky implement two alternative corrections to improve the TFD equation. In the first they assume that the correlation energy is local, i.e., it is a function of the electron density at a given radius, but do not numerically integrate the resulting TFD-like equation but rather obtain approximate solutions. In their second approach the correlation effect is treated in an average way. A mean correlation correction to the pressure based on the average electron density in the cell is added to the usual TFD surface pressure. They find that this latter method agrees considerably better with experimental data in most cases. In a later paper²⁴ the correlation corrected equation of state is applied to the determination of the mass-radius relation for planets and cold, white dwarfs.

Ebina and Nakamura²⁵ carry out a similar calculation and find that Salpeter and Zapolsky overestimate the effect of correlation in their approximate local calculation and even more so in their average treatment. Even with the addition of correlation, the unphysical aspects of the TFD model remain in these equation of state calculations. Near the origin of each cell the electron density blows up and zero pressure TFD cells are identical with TFD atoms.

A further refinement of the equation-of-state calculation can be made by employing the TFD- λ W statistical model in conjunction with the Wigner-Seitz spherical-cell approximation. Several authors have performed calculations of this sort. Perrot²⁶ solves the TFD- $\frac{1}{9}$ W model as a fourth-order ordinary differential equation (ODE) and gives results for several elements for fairly low compres-

sions. In a second paper²⁷ he generalizes his results for low, finite temperatures. In this case the gradient correction is a function of electron density. More²⁸ does a detailed study of aluminum in the TFD- λ W model. He compares against augmented-plane-wave (APW) band-structure calculations and looks at the effect of varying the Weizsacker term. He finds that $\lambda=0.483$ gives the best fit (with the APW calculations) for the electron structure near the nucleus. Yonei, Ozaki, and Tomishima²⁹ consider an iron atom in a heat bath and investigate the effects of exchange correlation and the Weizsacker correction over a wide range of temperatures and compressions. These calculations are relevant to hot dense plasmas. Yonei³⁰ employs a simple relativistic correction to TFD- λ W theory: The kinetic energy functional is modified but relativistic corrections to the Weizsacker and exchange terms are neglected. The high-pressure equation of state for iron and gold is calculated using a Weizsacker coefficient $\lambda=\frac{1}{5}$ (again because of the good fits it gives to atomic energies) and finds that relativistic effects are indeed important, as expected, but only at very high compressions.

In this paper we apply the nonrelativistic TFD- λ W model to calculate the cold equation of state for several elements. Of greatest interest to us are the elements and parameter range appropriate to matter in cold, degenerate stars like white dwarfs. Though our physical model is highly idealized, our numerical code is rugged and can achieve high accuracy with modest resources. It can also be extended in a straight forward manner to treat multidimensional cases (i.e., nonspherical lattice cells). We show that the inhomogeneity correction removes the major physical defects of the TFD lattice electronic structure. Atoms are infinite and zero-pressure cells are true *condensed* states. More significantly, the TFD- λ W model improves the equation of state at very low pressure, bringing the theoretical results into closer agreement with experimental data. We examine the effect of varying the Weizsacker coefficient λ . As expected, the Weizsacker coefficient λ , required to obtain good agreement with experiment, decreases as heavier atoms (with higher electron density) are considered. Similarly, TFD- $\frac{1}{9}$ W theory performs best (in computing zero-pressure densities) for elements with outer electron shells that are either almost empty or almost closed.

In another paper³¹ we plan to repeat our calculations with the TFD- λ W model supplemented with correlation corrections and compare our results with more sophisticated treatments based on integrating the Kohn-Sham equations. (The latter account for the effects of shell structure, which are important for finite Z at the very lowest pressures.³²) We conclude that the gradient correction alone represents a very substantial improvement to the low-pressure equation of state. The TFD- λ W model is both empirically and theoretically well motivated. It is straightforward to implement in any calculation involving an equation of state, particularly when a large dynamic range of density it required (e.g., for stellar structure calculations). In a planned paper³³ we use a similar model to study high- Z matter in the presence of very high magnetic fields relevant to neutron star atmo-

spheres.

In Sec. II we present the basic equations of the TFD- λ W statistical model and specialize them to the case of a spherically symmetric Wigner-Seitz lattice cell. In Sec. III we discuss our numerical method and describe checks on the accuracy of our lattice solutions and pressure computations. In Sec. IV we present numerical results for our equation of state and compare them with low-pressure data for several elements. We also calculate low-mass, equilibrium stellar models based on the TFD- $\frac{1}{9}$ W and the TFD- $\frac{1}{5}$ W equations of state for carbon and compare them with earlier calculations.

II. BASIC EQUATIONS

A. TFD- λ W model

The total energy in the TFD- λ W statistical model may be written³⁴ as a linear sum of kinetic, potential, and exchange components $E = E_k + E_p + E_a$. The kinetic energy is written as a sum of the plane-wave electron contribution and the inhomogeneity correction term of Weizsacker (we use atomic units $\hbar = m_e = e = 1$ throughout)

$$E_k = \int \left[\kappa_k n^{5/3} + \lambda \kappa_i \frac{(\nabla n)^2}{n} \right] d^3 \mathbf{r}, \quad (1)$$

where $n(\mathbf{r})$ is the electron number density and λ the gradient coupling coefficient. The potential energy is

$$E_p = - \int \left[\frac{Z}{r} + \frac{1}{2} V_e \right] n d^3 \mathbf{r}, \quad (2)$$

where Z is the ion charge and

$$V_e = - \int \frac{n(\mathbf{r}')}{|\mathbf{r} - \mathbf{r}'|} d^3 \mathbf{r}' \quad (3)$$

is the electron potential. The Dirac exchange energy is

$$E_a = - \int \kappa_a n^{4/3} d^3 \mathbf{r}. \quad (4)$$

The numerical coefficients appearing above are $\kappa_k = \frac{3}{10} (3\pi^2)^{2/3}$, $\kappa_i = \frac{1}{8}$, and $\kappa_a = \frac{3}{4} (3/\pi)^{1/3}$. With the constraint that $\int n d^3 \mathbf{r} = Z$ (i.e., a Wigner-Seitz cell must be neutral), minimization of the total energy with respect to the variation of n leads to the variational principle

$$\delta E + V_0 \delta Z = 0, \quad (5)$$

where V_0 is a constant Lagrange multiplier. This variational equation results in the master equation for the TFD- λ W model

$$\begin{aligned} \frac{5}{3} \kappa_k n^{2/3} - 2\lambda \kappa_i \left[\frac{\nabla^2 n}{n} - \frac{1}{2} \frac{(\nabla n)^2}{n^2} \right] \\ - V - \frac{4}{3} \kappa_a n^{1/3} + V_0 = 0, \end{aligned} \quad (6)$$

where

$$V = \frac{Z}{r} + V_e \quad (7)$$

is the total electrostatic potential.

Consider the appropriate boundary conditions that we must now impose on Eq. (6). We adopt the Wigner-Seitz spherical-cell approximation, which, e.g., produces excellent agreement with calculations of Madelung (Coulomb) energies of bcc, fcc, and hexagonal lattices at high pressures.²² To implement this we assume that the charge is spherically distributed about the nucleus and at the boundary of the cell, $r = r_0$, we impose the symmetry condition $dn/dr = 0$. We also assume that the density is regular at the origin (i.e., n is finite as $r \rightarrow 0$).

With the standard substitutions $y = rn^{1/2}$ and $U = rV$ we arrive at the form of Eq. (6) that we solve numerically:

$$\begin{aligned} 4\lambda \kappa_i \frac{d^2 y}{dr^2} - \frac{5}{3} \kappa_k r^{-4/3} y^{7/3} \\ + \frac{4}{3} \kappa_a r^{-2/3} y^{5/3} + \left[\frac{U}{r} - V_0 \right] y = 0. \end{aligned} \quad (8)$$

The corresponding boundary conditions are

$$y = 0 \text{ at } r = 0, \quad \frac{dy}{dr} = \frac{y(r)}{r} \text{ at } r = r_0. \quad (9)$$

Equation (8) for the density function $y(r)$ must be solved self-consistently with the potential function $U(r)$. The potential is given by Eqs. (3) and (7) which, using Poisson's equation, may be rewritten,

$$U = 4\pi \left[\int_r^{r_0} y^2 dr' - r \int_r^{r_0} \frac{y^2}{r'} dr' \right], \quad (10)$$

under the total charge constraint

$$Z = 4\pi \int_0^{r_0} y^2 dr \quad (11)$$

for a neutral cell. Equation (1) guarantees that both the electric potential and electric field are zero at the boundary of a cell. When Eq. (11) is satisfied, it also ensures that $V \rightarrow -Z/r$ as $r \rightarrow 0$. The matter density ρ in the Wigner-Seitz approximation is given by

$$\rho = \frac{A m_B}{4\pi r_0^3 / 3} = \frac{A}{Z} m_B \bar{n}, \quad (12)$$

where A is the atomic weight of the nucleus, m_B is the baryon rest mass (in units of m_e), and \bar{n} is the mean electron number density in a cell.

B. The pressure

Once we have solved for the electronic structure of a cell we have three computationally different, but mathematically equivalent, ways of obtaining the pressure. For cold matter the first law of thermodynamics gives $P = -dE/d\mathcal{V}$, where dE is the change in the energy of the Wigner-Seitz cell induced by a change in its volume $d\mathcal{V}$, keeping the charge fixed. Direct numerical implementation of this equation in the form of a finite

difference $P = -\Delta E / \Delta V$ requires calculation of at least two neighboring cell models (see Sec. III). Alternatively, it is possible to derive formulas for the pressure based only on local quantities at the cell surface

$$P = \left(\frac{2}{3} \kappa_k n^{5/3} - \frac{1}{3} \kappa_a n^{4/3} - 2\lambda \kappa_i \nabla^2 n \right)_{r_0} \quad (13)$$

$$= \left(\kappa_a n^{4/3} - \kappa_k n^{5/3} - V_0 n \right)_{r_0}. \quad (14)$$

(See the Appendix for a derivation.) In the limit $\lambda=0$ the surface formula (13) reduces to the familiar results for the TFD case^{19,34,20}. Equation (13) may also be written as

$$f \equiv \frac{P}{P_0} = 1 - \frac{5}{4} (3\pi^5 n)^{-1/3} \left[1 + (3n^4 / \pi)^{-1/3} \lambda \nabla^2 n \right]_{r_0}, \quad (15)$$

where $P_0 = \frac{2}{3} \kappa_k n^{5/3}$ is the pressure of an ideal, uniform electron gas.

Finally, a third way to get the pressure is to use the linear-scale-factor method³⁵ to obtain a global virial relation

$$\frac{3}{2} P \mathcal{V} = \frac{1}{2} (E_p + E_a) + E_k, \quad (16)$$

where $\mathcal{V} = 4\pi r_0^3 / 3$ is the cell volume. This formula is also derived in the Appendix. It reduces to the usual virial relation for a free atom when $P=0$.

III. NUMERICAL METHOD

In our numerical solution of the nonlinear TFD- λW system we have found it most effective to work with the linearized version of Eq. (8). Letting $y = y_0 + \Delta y$ with Δy small yields the linear form

$$\begin{aligned} 4\lambda \kappa_i \frac{d^2 y}{dr^2} - \left[\frac{35}{9} \kappa_k r^{-4/3} y_0^{4/3} \right. \\ \left. - \frac{20}{9} \kappa_a r^{-2/3} y_0^{2/3} - \left[\frac{U}{r} - V_0 \right] \right] y \\ = -\frac{20}{9} \kappa_k r^{-4/3} y_0^{7/3} + \frac{8}{9} \kappa_a r^{-2/3} y_0^{5/3}, \quad (17) \end{aligned}$$

which we finite difference using a standard second-order scheme and solve by iteration. Our radial grid typically consists of 1000 points. We find that for the most accurate calculation of pressure it is best to arrange the grid such that half of the available grid zones are placed with uniform spacing out to a radius of $0.05r_0$ - $0.15r_0$ from the origin. The other half are joined on smoothly and distributed out to r_0 with an arithmetically increasing grid separation.

Our procedure for solving the fundamental coupled system consisting of Eqs. (8) and (10) follows closely that of Tomishima and Yonei¹⁰ and Yang.⁸ We begin with an initial density profile guess, y_{00} , which we take to be an exponential with a scale length appropriate for a TFD- λW atom ($r_0 = \infty$). We then calculate the potential, U_0 using Eq. (10). With this value of U_0 we guess a value of the Lagrange multiplier V_0 and solve Eq. (8) by iterating Eq. (17); each iteration requires solution of a simple tridiagonal system. When Eq. (17) has converged to a new

value of the density y_{01} we calculate the total charge. If the charge represented by y_{01} differs from Z , the desired nuclear charge, we choose a new value for V_0 and repeat the procedure until the total charge represented by some y_{0n} converges to Z . Note that the potential is kept fixed at its original value U_0 through this part of the procedure. We then form a new guess for the density function taking a linear combination of the form⁸

$$y_{10} = 0.7y_{00} + 0.3y_{0n}. \quad (18)$$

From y_{10} we compute U_1 and repeat the above iteration scheme to find a consistent y_{1n} and V_0 . This process continues until y_{N0} and y_{N-10} converge, yielding the desired solution for electron structure. It is interesting to note that the stability and rate of convergence depend rather sensitively on the coefficients appearing in Eq. (18).

Several tests were used to determine the accuracy of the code. First, by performing runs at several grid resolutions we verified that our implementation of the finite difference scheme was indeed accurate to second-order in the range of grid sizes between 500 and 10000 points. We then made detailed comparisons with the tabulated electronic structure given by Tomishima and Yonei¹⁰ for neon atoms (by putting our outer boundary at a very large value $r_0=15$) and found agreement to within 0.02%. We also compared with Yang's⁸ table of total energies of neon for different values of λ and found agreement to similar accuracy in all cases.

As we wished to make detailed comparisons with TFD lattices, we also constructed a code to repeat the FMT calculations. Their model only requires a straightforward ODE integration, thanks to the simple algebraic relation between the charge density and the potential in TFD theory. We carefully checked that in the limit $\lambda \rightarrow 0$ the results from our full TFD- λW calculations agreed with those from TFD (see Fig. 1). We also verified that our

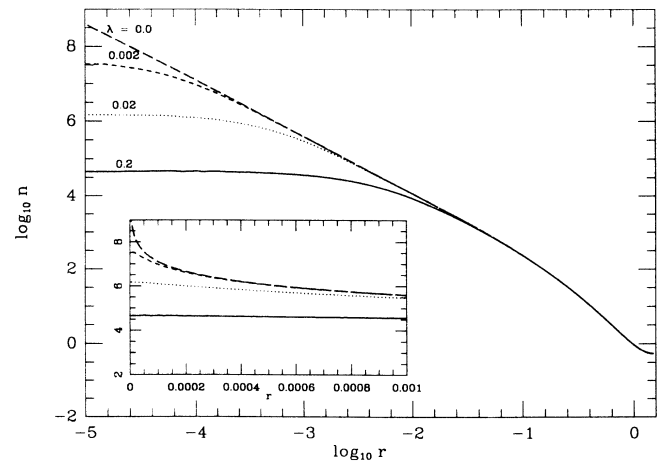


FIG. 1. The electron density as a function of radius (both in atomic units). Profiles are computed using TFD- λW theory for Wigner-Seitz cells of ^{56}Fe with radius $r_0=1.5$. Curves are shown for four different values of λ , the Weizsacker coupling constant. The inset shows the near-origin behavior.

three different methods for calculating the pressure all yielded the same result. By calculating the energy of two different sized cells one may use the first law, $P = -\Delta E / \Delta V$, to obtain the pressure. This result can be compared against the surface formula and the virial based calculation. We found that, as expected, all three methods converged to second order. However, for a given grid resolution the surface formula was by far the most accurate, especially for low densities at which $P \rightarrow 0$. The reason for this is that both the virial and first law formulas involve taking the small differences of large numbers obtained from integrals over the entire electron structure. The kinetic and potential energies must be calculated with extremely high precision for these methods to give correct results as $P \rightarrow 0$.

IV. NUMERICAL RESULTS

A. Equation of state

Consider the defect in TFD theory electronic structure near the nucleus. In Fig. 1 we plot the electron density as a function of radius for Wigner-Seitz cells of radius $r_0 = 1.5$ for ^{56}Fe . Curves are shown for four values of λ . Clearly for this medium density cell ($\rho = 45 \text{ g cm}^{-3}$) the structure near the cell boundary is similar, but the four cases diverge considerably near the nucleus. As λ approaches zero the electron density at the nucleus becomes greater and the turnover to constant density at $r = 0$ occurs at smaller values of r . In the limiting TFD case $\lambda = 0$, the density is obviously diverging as $r \rightarrow 0$. Note that the electron density at the outer boundary becomes slightly smaller as λ is decreased so all the cells have the same value of total charge.

In Fig. 2 we show the variation of the electron density profile and pressure with cell radius for ^{12}C . Results are plotted for the TFD- $\frac{1}{5}$ W model. As the cell radius r_0 is decreased (i.e., as the mass density increases) the electron density profile becomes more and more homogeneous [Fig. 2(a)]. At sufficiently small r_0 , it approaches a uniform electron gas. In Fig. 2(b) we plot the dimensionless pressure parameter f , defined by Eq. (15), as a function of the cell's mass density for the TFD- $\frac{1}{5}$ W and TFD- $\frac{1}{9}$ W models. As expected the function f approaches unity as the mass density increases and the density profile becomes increasingly uniform. The corresponding pressure curve for TFD theory is also shown for comparison. The curves converge as ρ becomes large.

In Fig. 3(a) we plot the equation of state for ^{12}C , ^{56}Fe , and ^{238}U calculated from both TFD theory and TFD- λ W theory with three different values of λ : $\frac{1}{3}$, $\frac{1}{5}$, and $\frac{1}{9}$. The choice $\lambda = \frac{1}{3}$ may be thought of as a reasonable upper bound; $\lambda = \frac{1}{5}$, the preferred value for free, closed-shell atoms, has good empirical support¹⁰ and is close to the value 0.186 obtained by Lieb² from the large- Z analysis; and $\lambda = \frac{1}{9}$ is the commonly accepted theoretical prediction of gradient expansion formalism.⁸ Also shown for comparison (the heavy solid lines and open points) are corresponding experimental data compiled from several sources.^{36,22,37} In Fig. 3(b) we exhibit the equation of

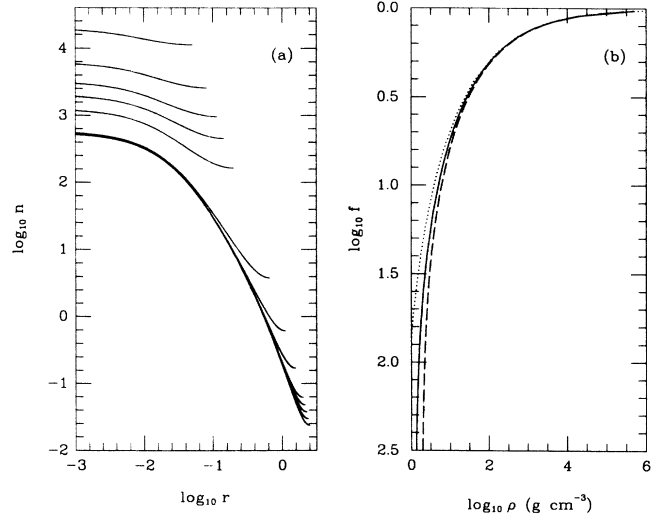


FIG. 2. (a) The electron density as a function of the radius (both in atomic units) for several ^{12}C Wigner-Seitz cells with varying radii, r_0 . The electron structure is calculated with TFD- $\frac{1}{5}$ W theory. Note that the density profiles become more and more uniform as the cells become smaller (higher mass density). (b) The nondimensional pressure function f as a function of matter density for ^{12}C . Curves are shown for calculations based on TFD (dotted curve), TFD- $\frac{1}{5}$ W (dashed curve), and TFD- $\frac{1}{9}$ W (solid curve) theory.

state over a larger mass density range and compare the results of TFD, TFD- $\frac{1}{9}$ W, and TFD- $\frac{1}{5}$ W. Clearly for carbon and iron, the TFD- λ W equation of state with $\lambda = \frac{1}{3}$ provides the best empirical fit to the low-pressure data including the limiting behavior as $P \rightarrow 0$. As the pressure increases all cells converge as the Weizsacker correction, as well as other interaction terms, diminish in relative importance. For uranium, the highest Z case, the agreement is best with $\lambda = \frac{1}{5}$.

It seems fairly evident that the λ necessary to get agreement with experiment at low pressures decreases as Z and, thus, the average electron density increases. The indication is that for cases where TF statistical theory in general is not very accurate—low Z and partially filled shell—increasing the value of λ can at least superficially improve results. If we compare the zero-pressure density predictions of Salpeter and Zepolsky,²² who used TFD with (unrealistically large) average correlation corrections with the results of TFD- $\frac{1}{5}$ W theory we find that the latter equation of state is slightly worse for iron (at low pressures) but better for uranium and considerably better for carbon.

It should be noted that our calculations are not strictly valid for uranium; the inner electrons become relativistic even for uranium atoms and our TFD- λ W model does not account for relativistic effects. Consider, for example, the magnitude of the nondimensional relativity parameter $x = p_f / m_e c$, which measures the degree to which a Fermi gas is relativistic. Here $p_f = (3\pi^2 n)^{1/3}$ is the electron Fermi momentum. Evaluating x for electrons near

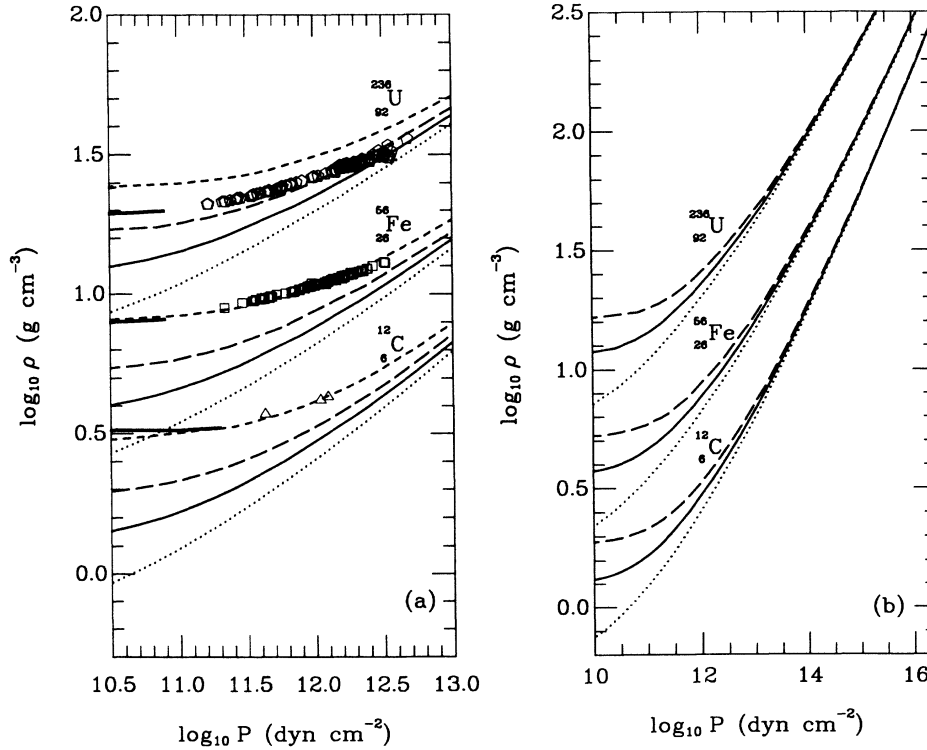


FIG. 3. (a) Theoretical equations of state are shown along with experimental data for ^{12}C (diamond data), ^{56}Fe and ^{236}U . For each element four theoretical equation-of-state curves are shown: TFD (dotted curve), TFD- $\frac{1}{9}\text{W}$ (solid curve), TFD- $\frac{1}{5}\text{W}$ (long-dashed curve), and TFD- $\frac{1}{3}\text{W}$ (short-dashed curve). The heavy solid lines are low-pressure data taken from Salpeter and Zapsolsky (Ref. 22) for uranium and iron and from Aleksandrov *et al.* (Ref. 37) for carbon. The open triangles, squares, and pentagons are high-pressure shock data from Marsh (Ref. 36). (b) This plot is similar to 3(a), showing a larger range of the equation of state. Curves for TFD (dotted), TFD- $\frac{1}{9}\text{W}$ (solid), and TFD- $\frac{1}{5}\text{W}$ (dashed) are shown.

the nucleus of a TFD- $\frac{1}{5}\text{W}$ zero-pressure uranium lattice cell gives $x = 2.73$, which is marginally relativistic. However, evaluating \bar{x} for the *mean* electron density inside r_0 gives $\bar{x} = 6.3 \times 10^{-2} r_0^{-1}$, which is quite nonrelativistic when $r_0 > \frac{1}{10}$. So it is not surprising that Engel and Dreizler¹⁵ show that the difference in total energy between a uranium atom calculated with a relativistic versus a nonrelativistic TFD- $\frac{1}{5}\text{W}$ model is only 4%. Similarly, since it can be computed from the *surface* density of electrons, the pressure is largely independent of whether or not the innermost electrons are relativistic.

Further support comes from calculations of Yonei.³⁰ He shows that the pressure difference between relativistic and nonrelativistic TFD- $\frac{1}{5}\text{W}$ calculations for gold at 500 g cm^{-3} (the highest compressions we graph for heavy elements) is only about 2%. We thus conclude that our nonrelativistic equation of state is fairly reliable, even for uranium, at low pressure and density, $\rho \leq 1 \times 10^3 \text{ g cm}^{-3}$.

In Table I we show the zero-pressure densities for several elements calculated with TFD- λW theory ($\lambda = \frac{1}{9}, \frac{1}{5}, \text{ and } \frac{1}{3}$) compared with results from TFD theory, TFD theory with average correlation corrections,²² and experi-

TABLE I. Zero-pressure densities (in g cm^{-3}) for seven elements are shown from experiment (Ref. 36) from TFD, from TFD with average correlation corrections (see Ref. 22), and from TFD- λW theory for several values of λ . Note that for TF, zero pressure occurs at zero density.

| Model | $^{12}_6\text{C}$ | $^{24}_{12}\text{Mg}$ | $^{56}_{26}\text{Fe}$ | $^{108}_{47}\text{Ag}$ | $^{197}_{79}\text{Au}$ | $^{207}_{82}\text{Pb}$ | $^{236}_{92}\text{U}$ |
|----------------------------|-------------------|-----------------------|-----------------------|------------------------|------------------------|------------------------|-----------------------|
| Experiment | 3.19 | 1.74 | 7.86 | 10.5 | 19.2 | 11.3 | 18.7 |
| TFD | 0.57 | 0.90 | 1.74 | 3.04 | 4.83 | 5.12 | 5.70 |
| TFD+correlation | 1.3 | 2.4 | 5.5 | 10.0 | 19.5 | 20.4 | 24.0 |
| TFD- $\frac{1}{9}\text{W}$ | 1.25 | 1.94 | 3.58 | 5.93 | 9.62 | 10.0 | 11.2 |
| TFD- $\frac{1}{5}\text{W}$ | 1.86 | 2.83 | 5.18 | 8.48 | 13.7 | 14.2 | 15.9 |
| TFD- $\frac{1}{3}\text{W}$ | 2.94 | 4.48 | 7.99 | 12.9 | 20.6 | 21.4 | 23.8 |

ment.³⁶ TFD- $\frac{1}{3}$ W theory is quite accurate for some elements but overall TFD- $\frac{1}{3}$ W is the most consistent; for the seven elements shown here TFD- $\frac{1}{3}$ W theory predicts the zero-pressure density with an average error (compared with experiment) of 32% compared with an average error of 39% for TFD- $\frac{1}{9}$ W theory and 68% for TFD theory. One also notes that TFD- $\frac{1}{9}$ W theory does best for the elements which have outer shells either nearly closed or nearly empty, ^{24}Mg and ^{207}Pb , and worst for ^{108}Ag and ^{197}Au which have partially filled outer shells. This is consistent with the view that $\lambda = \frac{1}{9}$ is exact in the high-electron-density limit and that TFD- λ W theory does not account for shell effects like spin-orbital coupling. In a forthcoming paper³¹ we plan to incorporate correlation corrections and repeat this comparison. A satisfactory theory must account for the experimental zero-pressure densities of all the elements. It is clear that, while the gradient correction greatly improves the agreement, it alone cannot consistently reproduce the zero-pressure laboratory data.

In TF and TFD theories in the Wigner-Seitz approximation, the lattice cell of zero pressure corresponds identically to the free-atom configuration. For TF, this cell, denoted by an asterisk, extends out to infinity ($r_0^* \rightarrow \infty$); the corresponding surface electron density n^* and lattice matter density ρ^* are both zero. For TFD, the $P=0$ cell occurs at a finite value of $r_0^* = r_0^*(Z)$, corresponding to a nonzero value of $n^*(r_0) = 2.13 \times 10^{-3}$ (in atomic units) and $\rho^* = \rho^*(A, Z)$. In both cases the electron density is automatically guaranteed to be smooth across the cell boundary [i.e., $n'(r_0) = 0$] for all $P \geq 0$ by virtue of the surface boundary condition $V'(r_0) = 0$.

In TFD- λ W theory, as in TFD, the zero-pressure lattice cell occurs at a finite value of $r_0^* = r_0^*(\lambda, A, Z)$ and, hence, a nonzero value of $n^*(r_0)$ and $\rho^* = \rho^*(\lambda, A, Z)$. However, by contrast with TFD, this Wigner-Seitz cell is not the free atom of TFD- λ W theory, since the latter extends to infinity with an exponentially decreasing electron density. Instead, the $P=0$ lattice is a truly *condensed* state of matter, distinct from the free atom, when the Weizsacker correction is included. Smoothness across neighboring cells [$n'(r_0) = 0$] is imposed by the surface boundary condition (9) on the second-order density equation. As in TFD, the TFD- λ W pressure P becomes negative in the range $r_0^* < r_0 < \infty$, so there is a density regime within $0 < \rho < \rho^*$ for which cells cannot exist. [The existence of a negative pressure domain at large r_0 and small, but nonzero, $n(r_0)$ is evident from Eq. (14), since $V_0 > 0$ for large cells.] However, $P=0$ when $r_0 = \infty$ and $n(r_0) = 0$ in TFD- λ W by Eq. (14), so that the free atom extending to infinity is well defined. At infinity the cell and atom boundary conditions are, of course, equivalent.

B. Applications to stellar models

Finally, we employ our equation of state to construct models of cold, spherical stars in hydrostatic equilibrium.

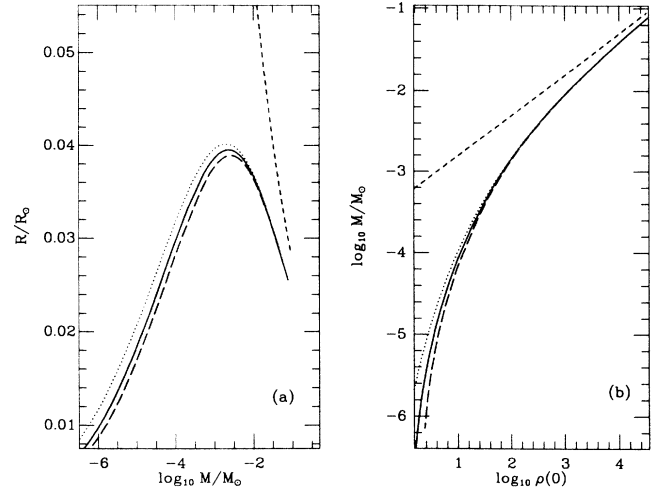


FIG. 4. (a) The mass-radius relation (in solar units) for cold ^{12}C equilibrium stars computed using the TFD (dotted curve), TFD- $\frac{1}{9}$ W (solid curve), and TFD- $\frac{1}{3}$ W (long-dashed curve) equations of state. The final curve (short-dashed) shows the result for an equation of state of ideal, cold, degenerate electrons ($P = P_0$, $A/Z = 2$). (b) The central density (in g cm^{-3}) is plotted against the mass for carbon stars computed using TFD (dotted curve), TFD- $\frac{1}{9}$ W (solid curve), TFD- $\frac{1}{3}$ W (long-dashed curve), and ideal electron (short-dashed curve) equations of state.

The Newtonian equilibrium equations are given by

$$\frac{dP(r)}{dr} = -G \frac{M(r)\rho(r)}{r^2}, \quad (19)$$

$$\frac{dM(r)}{dr} = 4\pi r^2 \rho(r), \quad (20)$$

where $M(r)$ is the mass interior to radius r . Equations (19) and (20) are integrated from the stellar center at $r=0$, where $M(0)=0$, $\rho=\rho(0)$, and $P=P(\rho(0))$, out to the surface at $r=R$, where $P=0=\rho$ and $M(r)=M$ (see Ref. 18 for detailed discussion and references on cold, degenerate stars). Figure 4(a) shows the resulting mass-radius relation for carbon white-dwarf models. Curves are shown for the TFD, TFD- $\frac{1}{9}$ W, and TFD- $\frac{1}{3}$ W equations of state. Figure 4(b) shows the relation between the central mass density $\rho(0)$ and the total mass. For comparison, the curves for models constructed from an ideal electron gas equation of state ($P = P_0$ and $A/Z = 2$) are plotted. These models are polytropes of index $\frac{3}{2}$ and correctly describe nonrelativistic stellar configurations of high density and pressure. We focus on carbon stars, since most white dwarfs are believed to be predominantly carbon.¹⁸ We find that the mass-radius relationship from TFD- λ W theory agrees very closely with that given by Zapolsky and Salpeter²⁴ for TFD with average correlation corrections. In particular, we find that for $\lambda = \frac{1}{9}$ the maximum radius of a carbon white dwarf is $R_{\text{max}} = 3.9 \times 10^{-2} R_{\odot}$, which occurs for a mass $M = 2.3 \times 10^{-3} M_{\odot}$.

ACKNOWLEDGMENTS

We would like to thank H. Bethe, L. Bildsten, L. S. Finn, D. Lai, E. E. Salpeter, M. Teter, H. Van Horn, and I. Wasserman for several helpful discussions. This work was supported by National Science Foundation Grant No. AST-87-14475 to Cornell University. Computations was performed at the Cornell National Supercomputer Facility, which is supported in part by the National Science Foundation, IBM Corporation, New York State, and the Cornell Research Institute. Financial support from the John Simon Guggenheim Memorial Foundation is also gratefully acknowledged by S.L.S.

APPENDIX: PRESSURE FORMULAS

First we derive a surface pressure formula following the derivation for TFD in the work of Gombas.³⁴ The pressure of a cell is given by the first law of thermodynamics as $P = -dE/d\mathcal{V}$. This may be computed as

$$P = -\frac{1}{4\pi r_0^2} \frac{\partial E}{\partial r_0} = -(\varepsilon)_{r_0} - \frac{1}{4\pi r_0^2} \int_0^{r_0} \frac{\partial \varepsilon}{\partial r_0} d^3\mathbf{r}, \quad (\text{A1})$$

where ε is the total energy density defined by $E = \int_0^{r_0} \varepsilon d^3\mathbf{r}$ with the total energy E given by Eqs. (1)–(4). For the TFD- λ W model energy this becomes

$$P = - \left[\kappa_k n^{5/3} - \kappa_a n^{4/3} - \left[\frac{Z}{r} + \frac{1}{2} V_e \right] n \right]_{r_0} - \frac{1}{r_0^2} \int_0^{r_0} r^2 dr \frac{\partial n}{\partial r_0} \left[\frac{5}{3} \kappa_k n^{2/3} - \frac{4}{3} \kappa_a n^{1/3} - \lambda \kappa_i \frac{(\nabla n)^2}{n} - \left[\frac{Z}{r} + \frac{1}{2} V_e \right] n \right] - \frac{1}{r_0^2} \int_0^{r_0} r^2 dr \left[\frac{\lambda \kappa_i}{n} \frac{\partial}{\partial r_0} [(\nabla n)^2] - \frac{1}{2} n \frac{\partial V_e}{\partial r_0} \right], \quad (\text{A2})$$

where we have used the boundary condition $\nabla n = 0$ at the cell surface in the first term. Using the relations

$$\int_0^{r_0} r^2 dr \left[n \frac{\partial V_e}{\partial r} \right] = r_0^2 V_e(r_0) n(r_0) + \int_0^{r_0} r^2 dr \left[V_e \frac{\partial n}{\partial r} \right] \quad (\text{A3})$$

and

$$\frac{1}{n} \frac{\partial}{\partial r_0} (\nabla n)^2 = 2 \nabla \cdot \left[\frac{\nabla n}{n} \frac{\partial n}{\partial r_0} \right] - 2 \frac{\nabla^2 n}{n} \frac{\partial n}{\partial r_0} + \frac{2}{n^2} (\nabla n)^2 \frac{\partial n}{\partial r_0}, \quad (\text{A4})$$

and using Eq. (6) we arrive at [the first term on the right-hand side of Eq. (A4) vanishes under integration]

$$P = - \left[\kappa_k n^{5/3} - \kappa_a n^{4/3} - \left[\frac{Z}{r} + V_e \right] n \right]_{r_0} + \frac{1}{r_0^2} \int_0^{r_0} r^2 dr V_0 \frac{\partial n}{\partial r_0}. \quad (\text{A5})$$

Using the fact that the total charge stays fixed when the cell is compressed gives us

$$\frac{\partial Z}{\partial r_0} = 0 = 4\pi \frac{\partial}{\partial r_0} \int_0^{r_0} r^2 dr n = 4\pi n(r_0) r_0^2 + 4\pi \int_0^{r_0} r^2 dr \frac{\partial n}{\partial r_0}, \quad (\text{A6})$$

which when substituted in Eq. (A5) leaves us with only surface terms. Upon another use of Eq. (6), we arrive at our final surface pressure formula Eq. (13). Substitution

of Eq. (6) again yields Eq. (14).

It is straightforward to derive the virial pressure formula (16), using the linear-scale-factor method of Fock.³⁵ Assume a contraction of a cell by a factor l^{-1} . The density then scales as $n_l(r) = l^3 n(lr)$. It is simple to show³⁵ that under such a contraction the total kinetic energy scales as $E_k^l = l^2 E_k$, the potential energy scales as $E_p^l = l E_p$, and the exchange energy scales as $E_a^l = l E_a$. For example, consider the Weizsacker contribution to the kinetic energy functional

$$E_{k_1} = 4\pi \lambda \kappa_i \int_0^R \frac{(\nabla n)^2}{n} r^2 dr. \quad (\text{A7})$$

For the contracted cell

$$E_{k_1}^l = 4\pi \lambda \kappa_i \int_0^{R/l} \frac{(\nabla_r n_l)^2}{n_l} l^2 r^2 dr. \quad (\text{A8})$$

With a change of variables $r' = lr$ this becomes

$$E_{k_1}^l = 4\pi \lambda \kappa_i \int_0^R \frac{[\nabla_{r'} n(r')]^2}{n(r')} l^2 r'^2 dr' = l^2 E_{k_1}. \quad (\text{A9})$$

We then have for the total energy

$$E^l = E_k^l + E_p^l + E_a^l = l^2 E_k + l E_p + l E_a. \quad (\text{A10})$$

Application of the first law,

$$dE^l = -P d\mathcal{V}^l, \quad (\text{A11})$$

gives us

$$2l E_k + E_p + E_a = 3l^{-4} P \mathcal{V}, \quad (\text{A12})$$

using the volume scaling relation $\mathcal{V}_l = l^{-3} \mathcal{V}$. Setting $l = 1$ in Eq. (A12) yields Eq. (16).

- *Also at Department of Astronomy and Department of Physics, Cornell University, Ithaca, New York 14853.
- ¹R. G. Parr and W. Yang, *Density-Functional Theory of Atoms and Molecules* (Oxford, New York, 1989).
- ²E. H. Lieb, *Rev. Mod. Phys.* **53**, 603 (1981).
- ³P. A. M. Dirac, *Proc. Cambridge Philos. Soc.* **26**, 376 (1930).
- ⁴H. Bethe and R. Jackiw, *Intermediate Quantum Mechanics* (Benjamin-Cummings, Reading, MA, 1968).
- ⁵N. Balazs, *Phys. Rev.* **156**, 42 (1967).
- ⁶E. H. Lieb and B. Simon, *Adv. Math.* **23**, 22 (1977).
- ⁷C. F. Weizsacker, *Z. Phys.* **96**, 431 (1935).
- ⁸W. Yang, *Phys. Rev. A* **34**, 4575 (1986).
- ⁹K. Yonei and Y. Tomishima, *J. Phys. Soc. Jpn.* **20**, 1051 (1965).
- ¹⁰Y. Tomishima and K. Yonei, *J. Phys. Soc. Jpn.* **21**, 142 (1966).
- ¹¹W. Jones and W. H. Young, *J. Phys. C* **4**, 1322 (1971).
- ¹²L. M. Kahn and S. C. Ying, *Surf. Sci.* **59**, 333 (1976).
- ¹³M. Brack, in *Density Functional Methods in Physics*, edited by R. M. Dreizler and J. da Providencia (Plenum, New York, 1985), p. 331.
- ¹⁴N. Stich, E. K. U. Gross, P. Malzacher, and R. M. Dreizler, *Z. Phys. A* **309**, 5 (1982).
- ¹⁵E. Engel and R. M. Dreizler, *Phys. Rev. A* **35**, 3607 (1987); **38**, 3909 (1988).
- ¹⁶H. Muller, E. Engel, and R. M. Dreizler, *Phys. Rev. A* **40**, 5542 (1989).
- ¹⁷K. Yonei, *J. Phys. Soc. Jpn.* **20**, 1051 (1971); E. K. U. Gross and R. M. Dreizler, *Phys. Rev. A* **20**, 1798 (1979).
- ¹⁸S. L. Shapiro and S. A. Teukolsky, *Black Holes, White Dwarfs and Neutron Stars: The Physics of Compact Objects* (Wiley, New York, 1983).
- ¹⁹R. P. Feynman, N. Metropolis, and E. Teller, *Phys. Rev.* **75**, 1561 (1949).
- ²⁰J. C. Slater and H. M. Krutter, *Phys. Rev.* **47**, 559 (1935); H. Jensen, *Z. Phys.* **111**, 375 (1983).
- ²¹B. K. Harrison *et al.*, *Gravitation Theory and Gravitational Collapse* (University of Chicago Press, Chicago, 1965).
- ²²E. E. Salpeter and H. S. Zapolsky, *Phys. Rev.* **158**, 876 (1967).
- ²³M. Gell-Mann and K. Brueckner, *Phys. Rev.* **106**, 364 (1957); M. Gell-Mann, *ibid.* **106**, 369 (1957).
- ²⁴H. S. Zapolsky and E. E. Salpeter, *Astrophys. J.* **158**, 809 (1969).
- ²⁵K. Ebina and T. Nakamura, *J. Phys. Soc. Jpn.* **52**, 1658 (1983).
- ²⁶F. Perrot, *Physica A* **98**, 555 (1979).
- ²⁷F. Perrot, *Phys. Rev. A* **20**, 586 (1979).
- ²⁸R. M. More, *Phys. Rev. A* **19**, 1234 (1979).
- ²⁹Y. Tomishima, *J. Phys. Soc. Jpn.* **54**, 1282 (1985); K. Yonei, J. Ozaki, and Y. Tomishima, *ibid.* **56**, 2697 (1987).
- ³⁰K. Yonei, *Phys. Lett. A* **138**, 193 (1989).
- ³¹A. M. Abrahams, D. Lai, and S. L. Shapiro (unpublished).
- ³²See, e.g., V. L. Moruzzi, J. F. Jank, and A. R. Williams, *Calculated Electronic Properties of Metals* (Pergamon, New York, 1978), and references therein; A. R. Williams and U. von Barth, in *Theory of the Inhomogeneous Electron Gas*, edited by S. Lundquist and N. H. March (Plenum, New York, 1983), p. 189.
- ³³A. M. Abrahams and S. L. Shapiro (unpublished).
- ³⁴P. Gombas, *Die Statistische Theorie des Atoms und ihre Anwendungen* (Springer, Vienna, 1949), p. 384.
- ³⁵The linear-scale-factor method to derive a virial relation is due to V. Fock, *Phys. Z. Sowjet.* **1**, 747 (1932), who considered a free atom $P=0$. The method was extended in Ref. 19 for a TFD atom under pressure and in Ref. 9 for a free TFD- λ W atom incorporating the Weizsacker gradient term.
- ³⁶S. P. Marsh, *LASL Shock Hugoniot Data* (University of California Press, Berkeley, 1980).
- ³⁷Low-pressure shock data for diamond may be found in I. V. Aleksandrov, A. F. Goncharov, A. N. Zisman, and S. M. Stishov, *Zh. Eksp. Teor. Fiz.* **93**, 680 (1987) [*Sov. Phys.—JETP* **66**, 384 (1987)].